EUROPEAN ORGANIZATION FOR NUCLEAR RESEARCH

Proposal to the ISOLDE and Neutron Time-of-Flight Committee

Study of the unbound proton-rich nucleus ^{21}Al with resonance elastic and inelastic scattering using an active target.

October 5, 2012

B. Fernández-Domínguez[1], O.Tengblad[2], M. Caamaño[1], H. Alvarez[1], J. Benlliure[1], W. N. Catford[3], J. Cederkäll[4], D. Cortina[1], F. Delaunay[5], P. Descouvemont[6], F. Farget[7], F. Flavigny[10], H. O. U. Fynbo[8], J. Gibelin[5], G. F. Grinyer[7], D. Loureiro[7], B. Jonson[9], E. Nacher[2], T. Nilsson[9], R. Orlandini[10], N. Orr [5], C. Paradela [1], J. Pancin[7], G. Randisi[10], R. Raabe[10], F. Renzi[10], K. Riisager[8], T. Roger[7], S. Sambi[10], D. Suzuki[11], N. Timofeyuk[3], J. S. Thomas[12], M. Vanderbrouck[11].

[1]*Universidade de Santiago de Compostela, 15754 Santiago de Compostela, Spain*
[2]*Instituto de Estructura de la Materia, CSIC, Madrid, Spain*
[3]*Department of Physics, University of Surrey, Guildford GU2 5XH, UK*
[4]*Department of Physics, Lund University, SE-221 00 Lund, Sweden*
[5]*LPC Caen, ENSICAEN, Université de Caen, CNRS/IN2P3, 14050 Caen, France*
[6]*PNTPN, C.P. 229, Université Libre de Bruxelles, B-1050 Brussels, Belgium*
[7]*GANIL, BP 55027, 14076 Caen Cedex 5, France*
[8]*Institut for Fysik og Astronomi, Arhus Univ., Arhus, Denmark.*
[9]*Fundamental Physics, Chalmers University of Technology, Goteborg, Sweden.*
[10]*Instituut voor Kern- en Stralingsfysica, K.U.Leuven, Celestijnenlaan 200d - B-3001 Leuven*
[11]*Institut de Physique Nucléaire, Université Paris-Sud-11-CNRS/IN2P3, France*
[12]*Schuster Laboratory, University of Manchester, Manchester, M13 9PL, UK*

Spokesperson: [B. Fernández-Domínguez, Olof Tengblad, M. Caamaño]
[beatriz.fernandez.dominguez@usc.es,olof.tengblad@csic.es,manuel.fresco@usc.es]
Contact person: [Jan Pawell Kurcewicz] [jan.kurcewicz@cern.ch]

CERN-INTC-2012-065 / INTC-P-366
05/10/2012

Abstract:

We intend to measure the structure of the unbound nucleus ^{21}Al via resonance elastic and inelastic scattering with an active target. There are many goals: a) to locate the $1/2^+$ level in ^{21}Al that brings information on the Thomas-Ehrman shift, b) to measure the energy spectrum of ^{21}Al which is a N=8 isotone with the resonance elastic scattering reaction, c) to investigate via inelastic scattering the strengh of core excitations in the existence of narrow unbound resonances beyond the proton drip-line.

Requested shifts: Total: 43 shifts (split into 1 runs over 1 year)
Installation: [2nd beamline (MAYA)]

1 Physics case

The structure of proton-rich nuclei at and beyond the drip-line exhibits very interesting phenomena such as: one-proton halo nuclei(^{8}B,^{12}N), two-proton emission (^{6}Be,^{18}Ne) and the presence of very narrow-resonance states built on a core in an excited state that could lead to unusual stable structures beyond the proton drip-line [1, 2].
Besides, exotic nuclei far away from stability show a large isospin asymmetry that modifies the residual interaction at the drip-lines. Symmetry breaking effects in proton-rich nuclei arise from the Coulomb interaction and by small charge-dependent parts of the strong interaction. In addition, the incorporation of three-body forces (3N) is expected to provide repulsive contributions to proton-rich nuclei [4] as seen in the case of the oxygen neutron-rich nuclei. Sizeable effects of these modifications are: 1) the Thomas-Ehrman Shift (TES), which produces a displacement in the energies of mirror nuclei, shift that becomes enhanced in low-l single-particle states of loosely-bound or unbound nuclei, 2) the ground-state energies and excitation spectra of proton-rich nuclei along the N=8 chain, where recent studies of chiral three-nucleon forces for the N=8 isotones place the ^{22}Si isotope at the proton dripline. [4], and 3) the widths of the resonance states that yield information on the excitation of the core. The N=8 shell gap in light medium-mass proton rich nuclei is only known up to ^{20}Mg, the next isotope in the chain is the ^{21}Al for which experimental information is not available. Following the LoI [3], we then propose to use the newly available 5.5 AMeV ^{20}Mg beam from HIE-ISOLDE together with an active target to populate unbound states of ^{21}Al through resonance-elastic and inelastic scattering up to $\simeq$ 4 MeV in excitation energy.

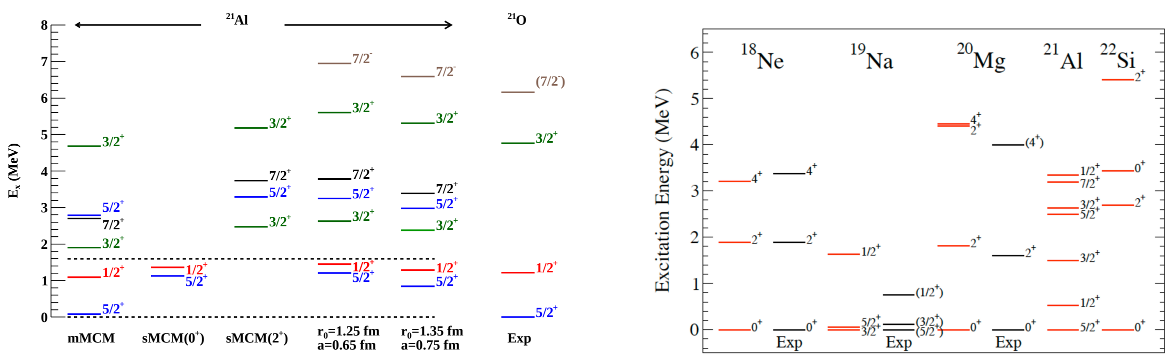

Figure 1: a) Energy Spectrum predicted in multi- and single-channel microscopic cluster model (MCM), and in two versions of the potential model. The spectrum of the mirror isotope ^{21}O is also shown [2]. b) Energy levels for the N=8 isotones calculated with NN+3N forces [4].

Very little is known about the structure of ^{21}Al which is proton unbound. Experimentally, only an upper limit of the half-life, $T_{1/2} < 35$ ns that corresponds to $\Gamma > 1.3 \times 10^{-8}$ eV, of the unbound ground state has been measured [5]. The theoretical predictions for the ground state binding energy show rather large discrepancies. The first theoretical predictions of the energies and widths of the resonance states in ^{21}Al have been made by N. Timofeyuk et al. [2] based on the mirror analog states in ^{21}O [6, 7]. The positions of the ^{21}Al resonances have been obtained using multi- and single-channel microscopic model (m/s MCM). The predictions for the ground and first excited states, $(5/2^+_1, 1/2^+_1)$, are rather different among the models. The energy of the ground state of ^{21}Al with the multi-channel MCM lies around 80 keV above the ^{20}Mg(0$^+$)+p threshold which is in disagreement with the half-life measurement of $T_{1/2} < 35$ ns. The single-channel model restores the agreement with the experiment, suggesting a large Thomas-Ehrman shift. The asymmetry in the energy spectrum between ^{21}Al-^{21}O calculated with the single-channel microscopic model, see Fig. 1 a), is bigger than the largest known Thomas-Ehrman shift observed in the ^{19}O($1/2^+_1$)-^{19}Na($1/2^+_1$) mirror pair (725 keV). Besides, the sMCM reproduces well the energies of other mirror pairs ^{21}Ne-^{21}Na and ^{19}O-^{19}Na. On the other hand, recent calculations by J. D. Holt [4], see Fig. 1 b), place the ground state at S_p = -2.46 and -1.69 for sd and sd$f_{7/2}p_{3/2}$ valence spaces, respectively. As it stands now, there are obvious discrepancies between the different models while the experimental measurements are lacking. Concerning the states above the ^{20}Mg(2$^+$)+p threshold, core excitations are expected to dominate the structure of the $3/2^+_1$, $5/2^+_2$ and $7/2^+_1$ states, as in its mirror nucleus ^{21}O. These states are predicted to be rather narrow because they are built on the first excited state of ^{20}Mg. In summary, we plan to study unbound states in ^{21}Al using resonance-elastic and inelastic scattering. There are many goals, the ^{20}Mg(p,p)^{20}Mg reaction will be used to scan the states coupled to the ^{20}Mg(0$^+$) state while the ^{20}Mg(p,p')^{20}Mg will investigate the states coupled to the ^{20}Mg(2$^+$) core. Recoil protons from the target will give information on the excitation function of the compound nucleus and the total path of the beam and fragment will be used to select the inelastic channel. Spectroscopic properties of the low-lying states will be obtained in a R-matrix analysis of the excitation function for a given angular range. In addition, angular distributions can be built since we explore a large angular coverage. This will allow us to gain further information on the shape of the resonances. Beyond the study of ^{21}Al adittional information on the ^{20}Mg+^{12}C channels is expected to be obtained simultaneously in the same experiment.

2 Experimental Method

The experiment will cover the energy range in the center of mass from Sp to 5.28 MeV. The ^{20}Mg beam will be delivered by the HIE-ISOLDE branch at 5.5 AMeV for an A/q ratio of 4.5 to the second beam line, where the active target set-up MAYA will be placed. The beam is expected to be produced with an isobaric contaminant ^{20}Na with a large ratio. MAYA is a detector [8] based on the active-target concept (see Fig. 2 a). This device allows to use a relatively thick target gas (27 x 27 x 31.4 cm) without loss of resolution. MAYA is equiped with a set of ancillary detectors, a wall of Silicon detectors of 20x20 cm and 700 μm thick, and 1 cm thick CsI scintillators at the back, to perform ΔE-E identification. A diamond detector will be situated at 0 degrees to stop the fragments reaching the end of the Volume of MAYA. A small drift chamber (DC) of 1.5 cm thick placed before the ancillary detectors will be used for position measurements of weak ionising particles. Previously, MAYA has been used at ISOLDE by R. Raabe [9] in 2012. In this succesful experiment the study of ^{13}Be through isobaric analog resonances was performed. For our experiment MAYA will be filled in with C_4H_{10} gas at roughly 98

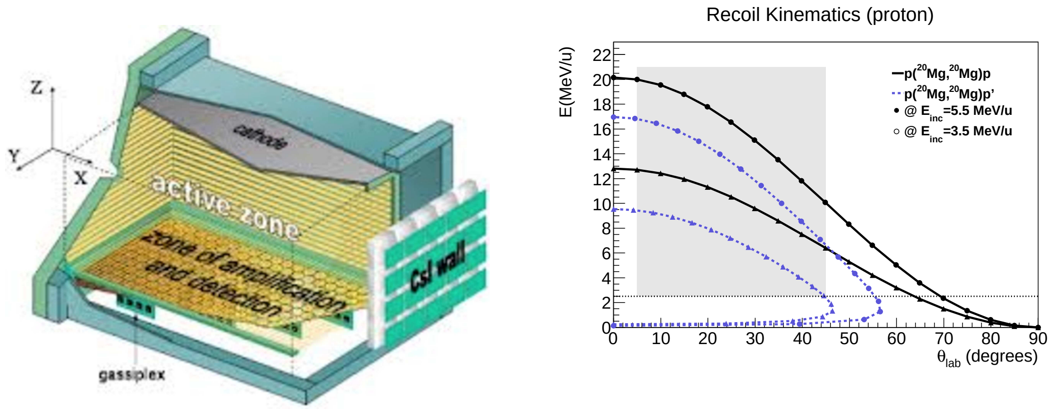

Figure 2: a) Schematic design of the active target MAYA. b) Kinematics of the recoil proton for the elastic (full line) and inelastic (dashed line) channels at two different energies E_{inc}=5.5 AMeV (full circles) and E_{inc} = 3.5 AMeV (full triangles). Shadowed area represents the average region recorded in the ancillary detectors DC-Si-CsI

mbar. The final value of the pressure will depend on the definitive amount of contaminants present in the experiment. The value of the pressure has been chosen with a twofold purpose a) to stop the beam in the gas to span excitation energies from $\simeq$ 4 MeV down to the ^{20}Mg(0^+)+p threshold and b) to remove the isobaric contaminant, ^{20}Na. The elimination of the isobaric contaminant is based on the different total paths travelled by each nucleus in the detector. The total path here is defined as the sum of two components: the beam path up to the point where the reaction takes place and the range of the produced fragment from the reaction point. The total path of ^{20}Mg varies between 23.5 and 31.4 cm while the total path of the isobaric contaminant ^{20}Na ranges from to 27.0 and 36.2 cm, this means that some ^{20}Na will also be present within the MAYA volume. However, they can be easily separated owing to the different total paths in MAYA. A correlation between the proton energy and the total path shown in Fig. 3 a) illustrates this purpose. The ^{20}Na nuclei with the longest total path will leave the MAYA volume and can be stopped in the veto detector placed at zero degrees. Consequently, an anti-veto coincidence will eliminate that part of the isobaric contribution.

Protons emitted at forward laboratory angles (θ_{lab}) between 5 and 45 degrees (see Fig. 2 b), from 170 to 90 in θ_{CM}, will be detected and identified through ΔE-E measurements in the DC-Si-CsI ancillary detectors. The excitation function will be obtained from the total kinetic energy (E) with a resolution of $\approx$ 200 keV in the laboratory, that becomes roughly $\approx$ 50 keV in the CM, and from the laboratory angle of the recoiling protons, with a resolution of $\approx 2\ ^o$ FWHM. However, in this experiment the θ_{lab} is not a direct observable since the particles do not ionise enough the gas, and hence the track of the particles can not be measured within MAYA. We will then use the position from the small drift chamber, that it is related with the angle, together with the energy-angle kinematical correlation at different beam energies to obtain the θ_{lab}. This method assumes that all the protons come from a specific channel for which we have calculated the kinematical correlation. Therefore, it is important to be able to separate the elastic and inelastic channels in the experiment. For that, we will use correlations between the energy of the protons

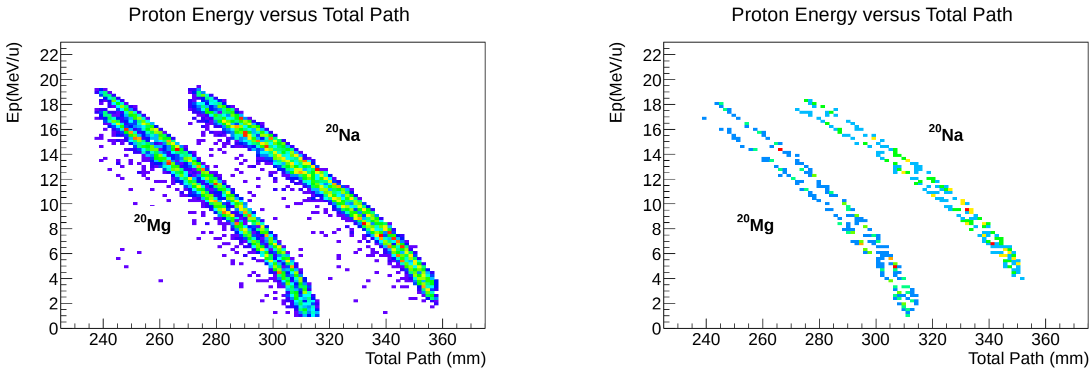

Figure 3: Energy proton versus the Total Path of ^{20}Na and ^{20}Mg in C_4H_{10} at 98 mbar. For each isotope the elastic channel corresponds to the band with the highest proton energy. a) Full range of positions b) For a position interval of 5 mm.

detected in the DC+Si+CsI and the total path of the beam-like partner. A simulation of the the Energy-Total Path correlation foreseen in this experiment is presented in Fig. 3 a) for the full range of positions covered by the ancillary detectors and b) for a given position within a 5 mm interval. A similar procedure was used previously in the following references [10] [11]. Fusion-evaporation background can be easily separated in MAYA owing to the different total path ranges of the compound nucleus.

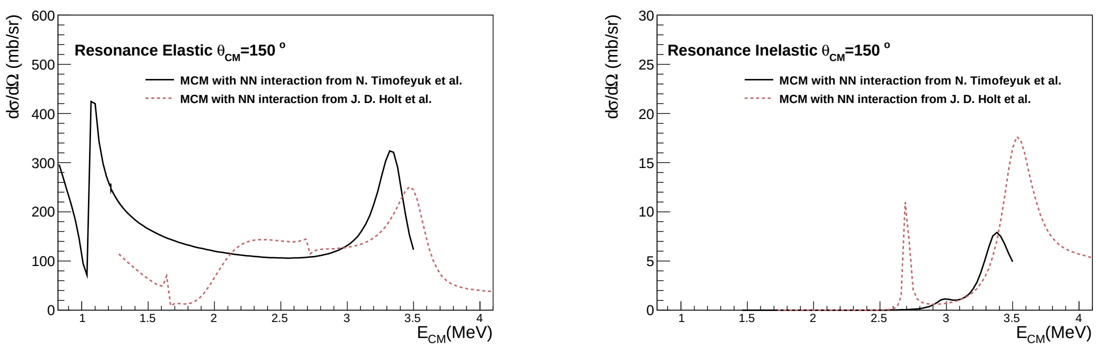

Figure 4: The calculated cross sections versus the energy in the center of mass E_{CM} with the MCM with NN interaction that reproduces $5/2^+$ and $1/2^+$ from N. Timofeyuk [2] (full-black line) and MCM with NN interaction that reproduces the sdpf results from J. D. Holt [4] (red-dashed line) a) For the elastic channel. b) For the inelastic channel.

The expected cross sections for $\theta_{CM} = 150\ ^o$ are shown in Figure 4 a) and b) for the elastic and inelastic channel respectively. The differences between the models will be clearly seen in our experiment with the current energy resolution. The excitation function will be built in steps of $\approx$ 50 keV in the E_{CM}, that corresponds to 4 mm of gas at $\approx$ 98 mbar pressure, which implies a target thickness of $N_i^{at} \approx 1.02$ x 10^{19} protons/cm^2. Assuming an average differential cross sections per energy bin of $< d\sigma_i^{elas,inelas}/d\Omega_{CM} >$ = 125 mb/sr and 5 mb/sr and for bins in the angular distribution of ± 15 degrees in the CM around $\theta_{CM} = 150\ ^o$, then the average cross section for each energy and angular bin is approximately $< \sigma_i^{elas,inelas} > = 203$ and 8.1 mb. For a beam intensity of ^{20}Mg of 50 pps and assuming 80% of MAYA efficiency, the counting rate per bin in 320 hours is shown in table 1.

Table 1: Table with the yields and uncertainties per angular and energy bin expected in this experiment. * The angular bin has been doubled for the inelastic channel.

Channel	Yield (c/h/bin)	Yield^{tot} (c/bin)	Error (%)
Elastic	3.0 x 10 $^{-1}$	100	10%
Inelastic*	2.5 x 10 $^{-2}$	10	30%

This counting time is adequate to distinguish between the two theoretical calculations and to give clear information on the spectroscopic properties of the states coupled to the ^{20}Mg(0^+). Concerning the inelastic channel we will double the angular bin in order to get $\approx$ 10 counts per bin, that corresponds to 30% uncertainty per bin. This would allow for reasonable measurements of the positions, widths and spin and parity of the resonances coupled to Mg(2^+) core.

3 Summary and counting rates

The proposed experiment is readibly feasible with MAYA provided a beam intensity of ^{20}Mg of 50 pps and a beam energy of 5.5 AMeV. As presented before, we could run with a large contribution from the isobaric contaminant ^{20}Na. However, the use of a stripper foil is also foreseen in order to remove as much of the contaminant as possible. We therefore request a total of 43 shifts of 8 hours.

3UT	of ^{20}Mg for tunning, pressure, and contaminant studies.
40UT	of ^{20}Mg for the scattering measurements.

Table 2: Requested beam time.

The number of shifts requested for this experiment has been calculated assuming a minimum of 50 pps of ^{20}Mg on MAYA. If the beam intensity happens to be less by a factor 5, that means 10 pps, the probability of measuring the inelastic channel will be minimal and the elastic channel will suffer from an increment in uncertainty (22%) for the same energy and angular bin. However, increasing the bin energy up to 100 keV in the E_{CM} will still give us reasonable information on the structure of ^{21}Al for which there is no experimental information available. The technique presented in this proposal with an active target opens new possibilities for performing resonance scattering measurements with very weak beams at ISOLDE where isobaric contaminants are present. Besides, a new prototype system ACTAR-TPC [12] incorporating a better energy and angular resolution as well as a faster electronics could also be envisaged for the measurement.

References

[1] L. Canton et al., Phys. Rev. Lett **59**, 33 (2006).

[2] N. Timofeyuk et al., Phys. Rev. C 86, 034305 (2012)

[3] M. J. G. Borge et al., CERN-INTC-2010-025-INTC-I-094. "Elastic resonance scattering study with a ^{20}Mg beam : p(^{20}Mg,p)^{21}Al"

[4] J. D. Holt et al., arXiv:1207.1509v1 [nucl-th]

[5] M. G. Saint-Laurent et al., Phys. Rev. Lett **59**, 33 (1987).

[6] B. Fernández-Domínguez et al. , Phys. Rev. C **84**, 011301(R) (2011).

[7] W. N. Catford et al, Nucl. Phys. A503, 263 (1989)

[8] C. E. Demonchy et al., Nucl. Instrum. Methods Phys. Res. A 573, 145 (2007).

[9] R. Raabe IS-203. INTC-Proposal 2010. "Study of ^{13}Be through isobaric analog resonances in the Maya active target".

[10] C. E. Demonchy Ph. D. Thesis, University of Caen (2003).

[11] T. Roger, Ph. D. Thesis, University of Caen (2009).

[12] ACTAR-TPC Conceptual Design Report. http://pro.ganil-spiral2.eu/spiral2/instrumentation/actar-tpc/actar-tpc-cdr-2012/view

Appendix

DESCRIPTION OF THE PROPOSED EXPERIMENT

The experimental setup comprises: (*name the fixed-ISOLDE installations, as well as flexible elements of the experiment*)

Part of the	Availability	Design and manufacturing
MAYA active-target detector	☒ Existing	☒ To be used without any modification ☐ To be modified
	☐ New	☐ Standard equipment supplied by a manufacturer ☐ CERN/collaboration responsible for the design and/or manufacturing
MAYA gas supply system	☒ Existing	☒ To be used without any modification ☐ To be modified
	☐ New	☐ Standard equipment supplied by a manufacturer ☐ CERN/collaboration responsible for the design and/or manufacturing

HAZARDS GENERATED BY THE EXPERIMENT (if using fixed installation:) Hazards named in the document relevant for the fixed [MINIBALL + only CD, MINIBALL + T-REX] installation.

Additional hazards:

Hazards	Maya active-target detector	Maya gas supply system	
Thermodynamic and fluidic			
Pressure	Isobutane (C_4H_{10}), $\approx$ 100 mbar, $\approx$ 20 l, flowing mode. Separation from the vacuum of the beam line with mylar window. An automatic safety valve will be installed on the beam line to prevent accidental escape of the gas.	Access to isobutane (one cylinder).	
Vacuum			
Temperature	room temperature (monitored)	room temperature	
Heat transfer			
Thermal properties of materials			
Cryogenic fluid			

Electrical and electromagnetic			
Electricity			
Static electricity	Static electric field in the detector typically 100 V/cm		
Magnetic field	[magnetic field] [T]		
Batteries	☐		
Capacitors	☐		
Ionizing radiation			
Target material [material]			
Beam particle type (e, p, ions, etc)	ions: ^{20}Mg, $T_{1/2}$= 90.8 ms, ^{20}Na, $T_{1/2}$= 447.9 ms		
Beam intensity	50 pps minimum		
Beam energy	5.5 MeV/u		
Cooling liquids	[liquid]		
Gases	[gas]		
Calibration sources:	☒		
• Open source	☐		
• Sealed source	☒ [ISO standard]		
• Isotope			
• Activity			
Use of activated material:			
• Description	☐		
• Dose rate on contact and in 10 cm distance	[dose][mSV]		
• Isotope			
• Activity			
Non-ionizing radiation			
Laser			
UV light			
Microwaves (300MHz-30 GHz)			
Radiofrequency (1-300 MHz)			
Chemical			
Toxic			
Harmful			
CMR (carcinogens, mutagens and substances toxic to reproduction)			
Corrosive			
Irritant			

Flammable	isobutane		
Oxidizing			
Explosiveness			
Asphyxiant			
Dangerous for the environment			
Mechanical			
Physical impact or mechanical energy (moving parts)			
Mechanical properties (Sharp, rough, slippery)			
Vibration			
Vehicles and Means of Transport			
Noise			
Frequency			
Intensity			
Physical			
Confined spaces			
High workplaces			
Access to high workplaces			
Obstructions in passageways			
Manual handling			
Poor ergonomics			

Hazard identification: Flammable gas: isobutane

Average electrical power requirements (excluding fixed ISOLDE-installation mentioned above): 1 kW